Bio-Medical Materials and Engineering 24 (2014) 271–277
DOI 10.3233/BME-130808
IOS Press

Gaussian fitting for carotid and radial artery pressure waveforms: comparison between normal subjects and heart failure patients

Chengyu Liu[a,b,*], Dingchang Zheng[c,*], Lina Zhao[a] and Changchun Liu[a]
[a]*School of Control Science and Engineering, Shandong University, Jinan, 250061, China*
[b]*School of Information Science and Engineering, Shandong University, Jinan, 250010, China*
[c]*Medical Physics Department, Newcastle University, Royal Victoria Infirmary, Newcastle Upon Tyne, NE1 4LP, UK*

Abstract. It has been reported that Gaussian functions could accurately and reliably model both carotid and radial artery pressure waveforms (CAPW and RAPW). However, the physiological relevance of the characteristic features from the modeled Gaussian functions has been little investigated. This study thus aimed to determine characteristic features from the Gaussian functions and to make comparisons of them between normal subjects and heart failure patients. Fifty-six normal subjects and 51 patients with heart failure were studied with the CAPW and RAPW signals recorded simultaneously. The two signals were normalized first and then modeled by three positive Gaussian functions, with their peak amplitude, peak time, and half-width determined. Comparisons of these features were finally made between the two groups. Results indicated that the peak amplitude of the first Gaussian curve was significantly decreased in heart failure patients compared with normal subjects (P<0.001). Significantly increased peak amplitude of the second Gaussian curves (P<0.001) and significantly shortened peak times of the second and third Gaussian curves (both P<0.001) were also presented in heart failure patients. These results were true for both CAPW and RAPW signals, indicating the clinical significance of the Gaussian modeling, which should provide essential tools for further understanding the underlying physiological mechanisms of the artery pressure waveform.

Keywords: Artery pressure waveform analysis, waveform matching, Gaussian function, heart failure

1. Introduction

The shape of artery pressure waveform is determined by the cardiac ejection and the mechanical and geometric properties of the systemic arteries [1]. Different cardiovascular parameters can be derived from the arterial pressure waveforms to indirectly evaluate the functions of the cardiovascular system, including the left ventricular systolic function, mechanical properties of arteries, and heart vasculature interaction. It is also generally accepted that the arterial pressure waveform includes a forward-travelling component generated by left ventricular ejection and some backward components [2]. Due to the pathological changes, arterial pressure waveforms in patients might differ from those in

* Corresponding authors: Tel / Fax: +86-531-88395384, E-mail: bestlcy@sdu.edu.cn and dingchang.zheng@ncl.ac.uk

normal subjects. Therefore, contour analysis of the arterial pressure waveform could be an important tool to explore the changes of cardiovascular system function [3].

Recently, the waveform fitting has become a promising method for contour analysis. It decomposes the arterial pulse waveform into different sub-waves. Logarithmic normal function [4, 5] and Gaussian function [6] have been used to model finger and toe photoplethysmographic (PPG) pulses. Both studies demonstrated reasonable effectiveness in modeling. In one of our recent publications, we systematically reported the accuracies and reliabilities of modeling both carotid and radial pulses by different numbers of Gaussian functions, and confirmed that using three positive Gaussian functions could achieve a very small residual error (less than 1.5%) [7]. In terms of its clinical significance, Rubins's study reported that the augmentation index and reflection index estimated by the Gaussian fitting method were highly related to those obtained by the traditional derivative method. However, only the peak timing information of the Gaussian curves was concerned in his study. The physiological relevance of other characteristic features, including the half-width and the peak amplitude of the modeled Gaussian curves, has been little investigated. Further studies on these features, as well as on their differences between normal subjects and patients, are thus required.

The aim of this study was to compare the characteristic features of Gaussian fitting for the carotid and radial artery pressure waveforms (CAPW and RAPW) between normal subjects and heart failure patients.

2. Methods

2.1. Subjects

One hundred and seven subjects aged between 25 and 75 years were studied. They consisted of 51 heart failure patients and 56 normal subjects, which were matched by age and sex. None of them have participated in any other 'clinical trials' within the previous three months. The study obtained a full approval from the Clinical Ethics Committee of the Qilu Hospital of Shandong University. All subjects gave their written informed consent prior to participation.

Heart failure patients were in Classes II-III of the New York Heart Association Functional Classification with LVEF<0.50 confirmed by an ultrasonic cardiogram (UCG) test. Healthy subjects had normal UCG, blood lipid and electrocardiogram (ECG). The subject demographic information is given in Table 1.

2.2. Signal Acquisition and Analysis

All the measurements were undertaken in a quiet, temperature-controlled (25 ± 3°C) measurement room at Shandong University Qilu Hospital. Before the formal recording, each subject lay supine on a measurement bed for 10 min to allow cardiovascular stabilization. All the measurements were performed by an experienced operator.

For each subject, the ECG, CAPW and RAPW signals were synchronously recorded for 5 min and converted into digital signals at a sample rate of 1000 Hz (Fig. 1). Off-line analysis was performed by a custom designed computer program developed by the MATLAB software. Firstly, the slow varying components (0-0.05 Hz) were removed from the ECG, CAPW and RAPW signals. Secondly, the R-wave peaks of the ECG were identified as reference points for detecting the corresponding feet (i.e., starting points) of the CAPW and RAPW signals [8]. The ectopic ECG beats were excluded [9].

Thirdly, the CAPW and RAPW signals were segmented using the starting points of two consecutive pulses (Fig. 1).

Next, the first 10 successive pulse segments without ectopic beats were selected for the subsequent analysis. Each pulse segment was normalized in period and amplitude, with the period to 1000 sample points, and the amplitude to unity between baseline and peak.

Table 1

Clinical variables from the normal subjects and heart failure patients.

Variables	Normal subjects	Heart failure patients	*P*-Values
No.	56	51	-
Men (%)	26 (46)	22 (43)	0.9
Age, year	58 ± 10	63 ± 9	0.1
Height, cm	169 ± 9	166 ± 8	0.4
Body mass, kg	71 ± 9	68 ± 9	0.5
Body Mass Index (BMI), kg/m^2	22.9 ± 3.1	23.8 ± 3.3	0.1
Heart Rate (HR), beats/min	70 ± 10	67 ± 8	0.4
Left Ventricular Ejection Fraction (LVEF), %	59 ± 12	38 ± 14	< 0.001

Note: Data are expressed as number or mean ± standard deviation (SD). *P*-values measure the separation between normal subjects and heart failure patients.

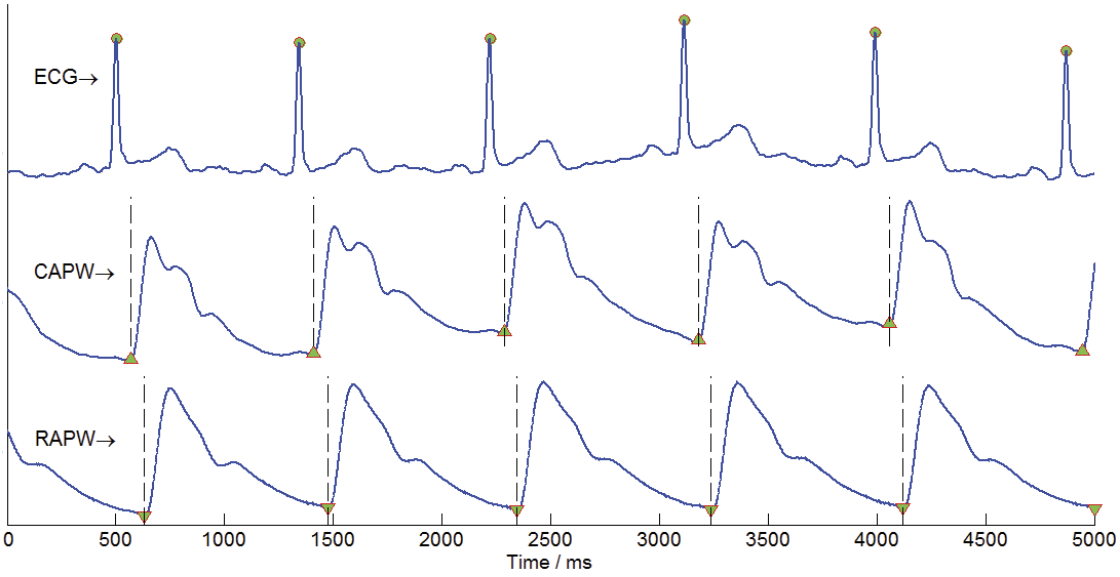

Fig. 1. An example of simultaneously measured ECG, CAPW and RAPW signals and the detected feature points.

2.3. Gaussian Fitting Method

Three positive Gaussian functions ($f_1^*(n)$, $f_2^*(n)$ and $f_3^*(n)$) were applied to each normalized pulse segment $f(n)$ (n=1,2,⋯,1000). They are defined as follows:

$$f_k^*(n) = H_k \times \exp\left(-\frac{2(n-n_k)^2}{W_k^2}\right) \qquad k = 1,2,3 \qquad n = 1,2,\cdots,1000\,, \tag{1}$$

where H_k denotes the peak amplitude, n_k denotes the peak time position and W_k denotes the half-width of each Gaussian curve.

Figure 2 demonstrates the Gaussian fitting for artery waveforms from a normal subject (A1 and A2) and a heart failure subject (B1 and B2). Nine characteristic features from three modeled Gaussian functions (peak amplitude, peak time and half-width) are also defined.

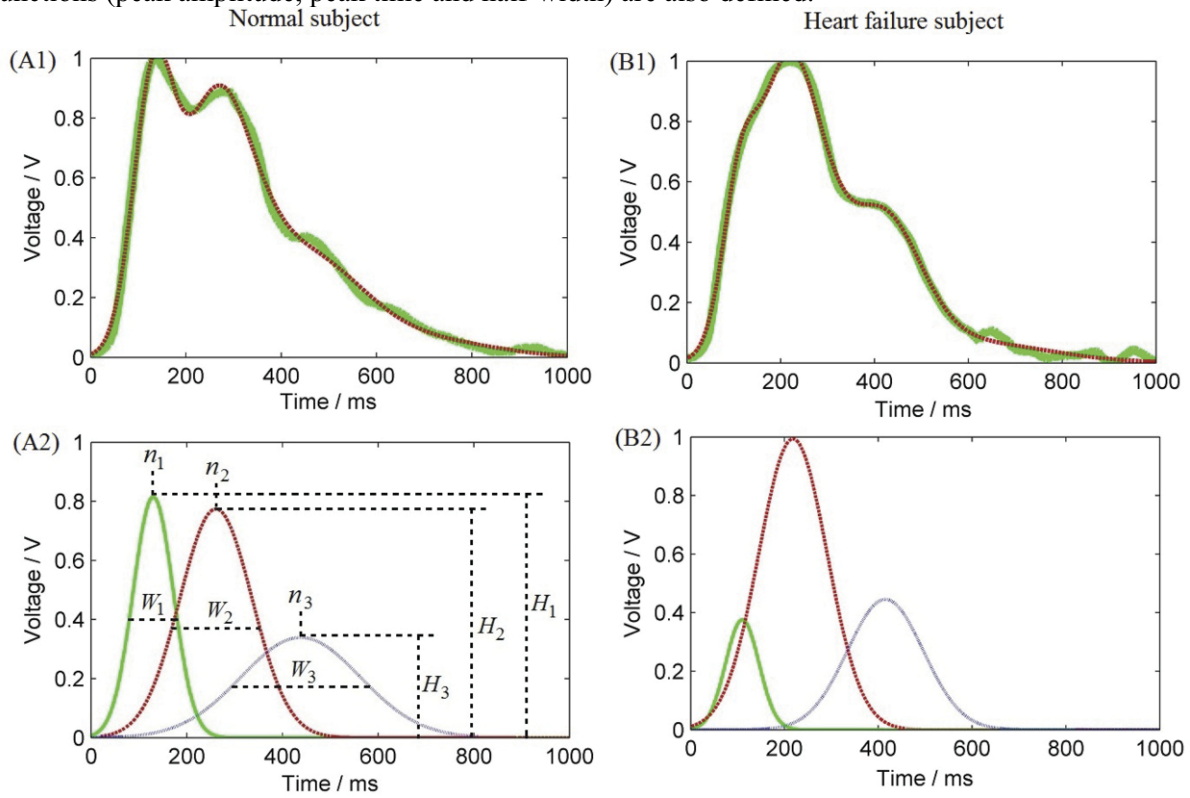

Fig. 2. Demonstration of Gaussian fitting for artery pulse waveforms: the normalized pulse segment $f(n)$ (solid green line) and the Gaussian fitting result (dash red line) from normal (A1) and heart failure subject (B1) are shown in the upper panels. The three corresponding Gaussian functions $f_1^*(n)$, $f_2^*(n)$ and $f_3^*(n)$ are shown in the bottom panels. The Guassian features: peak amplitude : H_1, H_2, H_3, peak time: n_1, n_2, n_3 and half-width: W_1, W_2, W_3 are also shown.

2.4. Evaluation of Gaussian Fitting

Nine parameters H_k, n_k and W_k (k=1, 2, 3) were determined for the three Gaussian functions applied. The least squares error (LSE) was used to assess the Gaussian fitting. It is calculated by

$$\mathrm{LSE} = \sum_{n=1}^{1000} \frac{[f_1^*(n) + f_2^*(n) + f_3^*(n) - f(n)]^2}{f^2(n)} \times 100\% \,. \tag{2}$$

A particle swarm optimizer was used to solve the optimization problem in Eq. (2) with the constrained condition $1<n_1<n_2<n_3<1000$ [10]. The parameter optimization will not be ceased until the LSE is smaller than 1.5%, which was accurate enough for the waveform matching.

2.5. *Statistical* analysis

The average characteristic features (peak amplitude, peak time and half-width) of the three modeled Gaussian curves were firstly calculated from 10 beats of each subject. Their overall values were then obtained across all subjects with the mean±standard deviation (SD) calculated. Student's *t*-test was used to compare the Gaussian feature differences between normal subjects and heart failure patients. Statistical significance was set a priori at $P<0.05$.

3. Results

Table 2 shows the comparison results of the nine Gaussian features between normal subjects and heart failure patients. For both CAPW and RAPW, in comparison with normal subjects, heart failure patients had significantly decreased peak amplitude of the first Gaussian curve, and significantly increased peak amplitude of the second Gaussian curve (all $P<0.001$).

It was also found that the peak times of the second and third Gaussian curves were significantly shorter in heart failure patients (both $P<0.001$), while there was no significant difference for the first Gaussian curve ($P=0.9$ for CAPW, and $P=0.7$ for RAPW). Consequently, as shown in Figure 3, the peak time interval between the first and second, and between the first and third Gaussian curves were significantly shorter in heart failure patients (all $P<0.001$).

In addition, only the half-width of the third Gaussian curve was significantly shorter in heart failure patients ($P<0.001$ for both CAPW and RAPW).

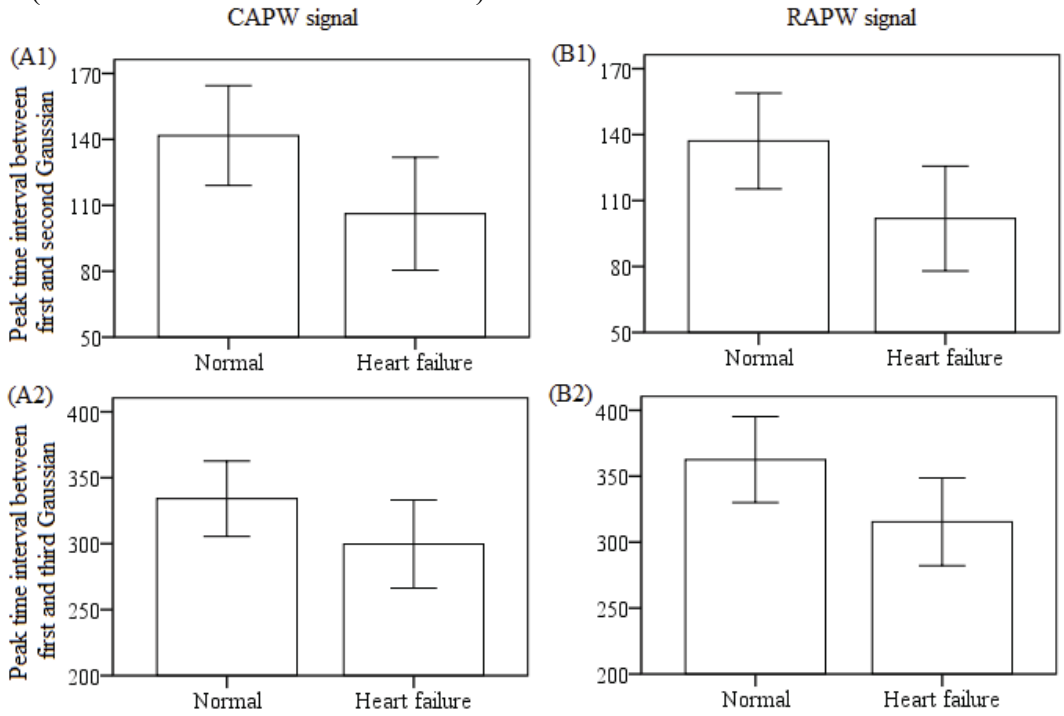

Fig. 3. Comparison of peak time intervals between two groups. Bar plots of peak time interval between the first and second, and between the first and third Gaussians for CAPW (A1 and A2) and RAPW (B1 and B2) signals are shown.

Table 2

Comparison of the characteristic features of the modeled Gaussian functions between normal subjects and heart failure patients.

Variables		CAPW			RAPW		
		Normal	Heart Failure	*P*-Values	Normal	Heart Failure	*P*-Values
Peak amplitude	H_1	0.81 ± 0.14	0.44 ± 0.16*	< 0.001	0.72 ± 0.13	0.53 ± 0.17*	< 0.001
	H_2	0.77 ± 0.11	0.92 ± 0.06*	< 0.001	0.70 ± 0.12	0.89 ± 0.08*	< 0.001
	H_3	0.42 ± 0.10	0.39 ± 0.12	0.5	0.48 ± 0.09	0.31 ± 0.11*	< 0.001
Peak time	n_1, ms	128 ± 12	126 ± 10	0.9	120 ± 11	125 ± 12	0.7
	n_2, ms	270 ± 11	232 ± 14*	< 0.001	257 ± 12	227 ± 11*	< 0.001
	n_3, ms	462 ± 19	425 ± 22*	< 0.001	483 ± 18	440 ± 21*	< 0.001
Half-width	W_1, ms	91 ± 12	90 ± 9	0.9	91 ± 11	89 ± 10	0.9
	W_2, ms	154 ± 13	149 ± 13	0.8	149 ± 13	157 ± 12	0.1
	W_3, ms	321 ± 27	238 ± 34*	< 0.001	365 ± 36	288 ± 31*	< 0.001

Note: Data are expressed as mean ± standard deviation (SD). * shows the statistical significance.

4. Discussion

This study extracted nine characteristic features from three modeled Gaussian functions for both CAPW and RAPW signals, providing the opportunities to investigate their physiological relevance and to explore the generation and reflection of the artery pressure waveforms. More importantly, the different Gaussian features between normal subjects and heart failure patients have been determined.

In the present study, the peak amplitude of the first Gaussian function was significantly lower in heart failure patients for both CAPW and RAPW signals. It is traditionally accepted that the arterial pressure waveform contains both forward and backward components [1, 2]. The forward component stems from the ejection of left ventricle, which is more likely to be linked with the first Gaussian function. Our results were consistent with that the contraction function of the left ventricle declines distinctly in heart failure patients.

We also found significantly shorter peak times of the second and third Gaussian functions in heart failure patients for both CAPW and RAPW signals. The backward component, which is possibly associated with the second and third Gaussian functions, could be caused by the reflection of the forward wave from sites of changes in impedance within the peripheral arterial system [11]. With the progress of heart failure, the central and peripheral arterial stiffness could be changed with different impedance matching between central aorta and peripheral arteries, resulting in a forward shift of the reflection wave [11, 12]. Additionally, the forward shift of the second and third Gaussians could also potentially lead to increases in the peak amplitudes. The significantly higher peak amplitude of the second Gaussian curve in heart failure patients has proven this point. In terms of the peak amplitude of the third Gaussian function, the fact of that difference between two groups only occurred in the RAPW signal but not in CAPW signal could be attributable to the different peripheral resistances.

In addition, the significantly shortened half-width of the third Gaussian function possibly indicated that the overall pressure waveform, especially in diastolic phase, had an obvious drop in heart failure patients.

The weak left ventricular contraction and the forward shift of back-travelling wave are regarded as the risk factors for the cardiovascular system [12, 13]. Using Gaussian fitting methods, these changes have been demonstrated in heart failure patients. Our study therefore confirmed that Guassian fitting can be a clinically useful method to analyse arterial waveform changes with diseases. It should be an

important step to further understand the underlying physiological mechanisms of the artery pressure waveform features.

5. Acknowledgements

This work was supported by the National Natural Science Foundation of China (61201049), the Hi-Tech Research and Development Program (863) of China (2009AA02Z408) and the China Postdoctoral Science Foundation (2013M530323).

References

[1] S.C. Millasseau, J.M. Ritter, K. Takazawa and P.J. Chowienczyk. Contour analysis of the photoplethysmographic pulse measured at the finger. *Journal of Hypertension* 24 **(**2006**)**, 1449-1456.

[2] S. Laurent, J. Cockcroft, L. Van Bortel, P. Boutouyrie, C. Giannattasio, D. Hayoz, B. Pannier, C. Vlachopoulos, I. Wilkinson and H. Struijker-Boudier. Abridged version of the expert consensus document on arterial stiffness. *Artery Research* 1 **(**2007**)**, 2-12.

[3] J. Allen and A. Murray. Age-related changes in peripheral pulse timing characteristics at the ears, fingers and toes. *Journal of Human Hypertension* 16 **(**2002**)**, 711-717.

[4] M. Huotari, A. Vehkaoja, K. Määttä and J. Kostamovaara. Photoplethysmography and its detailed pulse waveform analysis for arterial stiffness. *Journal of Structural Mechanics* 44 **(**2011**)**, 345-362.

[5] M. Huotari, A. Vehkaoja, K. Määttä and J. Kostamovaara. Pulse waveforms are an indicator of the condition of vascular system. In: *Proceedings of World Congress on Medical Physics and Biomedical Engineering,* 2012, pp. 526-529.

[6] U. Rubins. Finger and ear photoplethysmogram waveform analysis by fitting with Gaussians. *Medical & Biological Engineering & Computing* 46 **(**2008**)**, 1271-1276.

[7] C.Y. Liu, D.C. Zheng, A. Murray and C.C. Liu. Modelling carotid and radial artery pulse pressure waveforms by curve fitting with Gaussian functions. *Biomedical Signal Processing and Control* 8 **(**2013**)**, 449-454.

[8] J.P. Martinez, R. Almeida, S. Olmos, R. A.P. and P. Laguna. A wavelet-based ECG delineator: evaluation on standard databases. *IEEE Transactions on Biomedical Engineering* 51 **(**2004**)**, 570-581.

[9] C.Y. Liu, L.P. Li, L.N. Zhao, D.C. Zheng, P. Li and C.C. Liu. A combination method of improved impulse rejection filter and template matching for identification of anomalous intervals in electrocardiographic RR sequences. *Journal of Medical and Biological Engineering* 32 **(**2012**)**, 245-250.

[10] R. Mendes, J. Kennedy and J. Neves. The fully informed particle swarm: simpler, maybe better. *IEEE Transactions on Evolutionary Computation* 8 **(**2004**)**, 204-210.

[11] J. Sugawara, K. Hayashi and H. Tanaka. Distal shift of arterial pressure wave reflection sites with aging. *Hypertension* 56 **(**2010**)**, 920-925.

[12] G.F. Mitchell, H. Parise, E.J. Benjamin, M.G. Larson, M.J. Keyes, J.A. Vita, R.S. Vasan and D. Levy. Changes in arterial stiffness and wave reflection with advancing age in healthy men and women: the framingham heart study. *Hypertension* 43 **(**2004**)**, 1239-1245.

[13] M.F. O'ourke and W.W. Nichols. Changes in wave reflection with advancing age in normal subjects. *Hypertension* 44 **(**2004**)**, E10-11.